Interaction of blackbody radiation with xenon Rydberg atoms

G. F. Hildebrandt, E. J. Beiting, C. Higgs, G. J. Hatton, K. A. Smith, F. B. Dunning, and R. F. Stebbings
Department of Space Physics and Astronomy, Rice University, Houston, Texas 77001
and Rice Quantum Institute, Houston, Texas 77001
(Received 24 November 1980)

Effects due to the interaction of 300 K background radiation with Xe(nf) Rydberg atoms are reported. Transitions to nearby d and g levels are observed. When the ambient photon density is reduced to that appropriate to liquid-nitrogen temperature by cooling the apparatus, a corresponding reduction in the transition rates to these levels is observed. The transition rates are found to be consistent with those predicted by use of quantum-defect theory.

The interaction of background radiation with highly excited atoms has been the subject of several recent investigations.[1-9] In an earlier paper[1] we reported the observation of effects that were attributed to the photoexcitation and photoionization of Rydberg atoms by 300 K background blackbody radiation (BBR). In this paper we confirm this interpretation by demonstrating that a reduction in the ambient photon density results in a corresponding decrease in the photoexcitation rate. In addition, we show that the time development of the populations of states produced by blackbody-induced photoexcitation agrees very well with that predicted theoretically.

The apparatus has been described in detail elsewhere,[10,11] and only a brief description will be given here. A beam of ground-state xenon atoms is formed in high vacuum by effusion through a multichannel glass array. A fraction of the beam is excited to the $^3P_0$ metastable level by electron impact. The xenon beam is then intersected at right angles by the output of a pulsed, tunable dye laser to photoexcite a fraction of the $^3P_0$ atoms to a selected high-lying nf state. The Rydberg atoms are created in zero electric field ($\lesssim 0.2$ V cm^{-1}) in a region bounded by two parallel copper wire mesh grids. After a known variable delay, during which time the laser excited nf atoms interact with the BBR, the Rydberg atoms present in the interaction region are analyzed using selective field ionization (SFI).[10] To accomplish this a large negative voltage ramp is applied to the lower grid, while the upper grid is held at ground potential. The increasing field between the grids, which typically rises from $0 \rightarrow 1000$ V cm^{-1} in 1 μsec, ionizes the xenon Rydberg atoms and accelerates the resulting free electrons to a Johnston particle multiplier. The output of the multiplier is amplified and fed to a time-to-amplitude converter (TAC). The TAC is started at the beginning of the ionizing voltage ramp and is stopped by the first electron pulse subsequently registered by the detector. The TAC output is fed into a standard multichannel-pulse analyzer. For sufficiently low count rates (less than 0.1 per laser pulse) the multichannel analyzer stores a signal proportional to the probability of a field ionization event per unit time during the 1-μsec ramp. Knowledge of the time dependence of the ionizing field strength then allows the probability of field ionization per unit field increment to be derived. Since atoms in different Rydberg states ionize at different electric-field strengths it is possible to infer from such SFI data the state distribution of the excited states initially present. For example, in Fig. 1 are shown SFI data obtained after allowing parent Xe($23f$) atoms to interact with room temperature 300 K background radiation for 7 μsec. Several distinct ionization features are evident, each of which can be correlated with a particular initial (zero-field) Rydberg state. Recent detailed

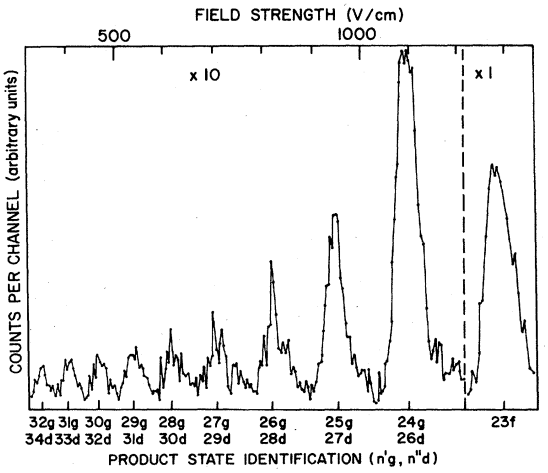

FIG. 1. SFI spectrum obtained after allowing Xe($23f$) atoms to interact with BBR at 300 K for 7 μsec. Ionization of parent $23f$ atoms yields the single large peak on the right. The BB features to its left (note × 10 magnification) are identified with the d and g states that contribute to each.

studies of field ionization[10, 12-15] have shown that in an increasing electric-field Rydberg atoms may follow a number of different paths to ionization, although in most cases either a predominantly diabatic or adiabatic path is followed. For the range of values of principal quantum number considered in this experiment ($20 \leq n \leq 34$), xenon Rydberg atoms with low l, and in consequence low values of $|m_l|$ at high fields,[16] show little evidence of diabatic behavior.

The large feature on the right of the SFI spectrum results from the adiabatic ionization of the parent Xe(23f) atoms. The smaller peaks to its left arise from the adiabatic ionization of the d and g states which result from BB induced photoexcitation from the parent state. The nd states of xenon have such large quantum defects that each $(n+2)d$ level is located between the n and $(n-1)$ hydrogenic Stark mainfolds. In consequence, $(n+2)d$ states ionize adiabatically at essentially the same field strengths as do ng states, which have negligible quantum defects. Each BB peak therefore results from the ionization of an ng and an $(n+2)d$ state and their identification is as indicated in Fig. 1.

To permit control of the thermal background radiation, the Rydberg excitation region is located in a copper box which can be cooled by liquid nitrogen, resulting in a controlled reduction of the ambient BB-photon density. The xenon and laser beams enter and exit through small apertures in the side of this box. Charged particles created in the interaction region exit the box through a small aperture, at the top, prior to detection by the multiplier. Copper-constantan thermocouples attached to the side and top of the copper box, and to the bottom grid, are used to monitor their temperature. Data were recorded both with the box at room temperature and with it cooled by liquid nitrogen, which resulted in a temperature in the range 80–90 K. Care must, however, be exercised to ensure that the photon density inside the cooled box is that appropriate to a blackbody at ~90 K. Room-temperature radiation leaks into the box through the holes necessary to allow the entry and exit of the laser and xenon beams and to allow electrons to reach the multiplier. If the inner walls of the box have a high reflectivity in the far infrared, as do many metal surfaces, a photon entering by one of these holes may undergo very many reflections before being absorbed or escaping, resulting in a photon density inside the box that is very nearly the same as outside. To remove this possibility, the inner surfaces of the box are lined with graphite coated copper wool, since auxiliary studies had shown this to be a good absorber in the far infrared. Calculations indicated that such an absorber would reduce the photon density inside the cooled box to within 10% of that appropriate to a blackbody at the same temperature.

The effect of reducing the background photon flux is illustrated in Fig. 2 for parent Xe(25f) atoms. The marked decrease in the number of higher-lying states evident upon reducing the ambient temperature provides direct evidence that these states are indeed populated by BB induced photoexcitation. This interpretation has been confirmed by measuring the BB induced transition rates at 300 and 90 K and comparing the ratio of these rates to that expected on the basis of blackbody spectral data and calculated transition rates.

The BB-induced transition rates are determined by measuring the time dependence of each BB feature. In order to determine this it is necessary first to recognize and subtract backgrounds due to effects such as Penning ionization or to f states populated by untuned laser fluorescence. The magnitude of these backgrounds is determined by tuning the laser between two adjacent f states. An additional background must be considered when analyzing the first BB peak to the left of the main peak. This results because a small fraction of the laser-produced nf atoms ionize at field strengths corresponding to this BB peak. Thus

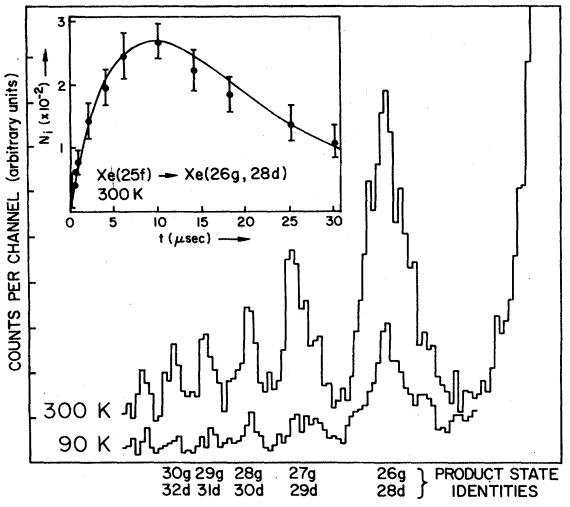

FIG. 2. Effect of reduced temperature on the size of BB features populated by photoexcitation of Xe(25f) atoms. The SFI spectra were obtained at 300 K (upper curve) and 90 K (lower curve). Both are normalized to the same Rydberg production at $t=0$, and both are taken at $t=9$ μsec. The inset shows the time development of the feature comprising 26g, 28d atoms at 300 K. The ordinate axis is normalized to unit Rydberg production at $t=0$. The solid line shows the fit to the data obtained using the single reservoir model.

at early times, when the BB population is small and the parent population large, parent-state ionization provides a small, but significant, contribution to this BB feature. However, knowledge of the detailed shape of the parent *nf* feature enables this contribution to be determined and subtracted.

The growth of the various blackbody induced features is properly described using a model in which each BB peak is treated as comprising *d* and *g* states, each populated at a different rate and each decaying with a different lifetime. In fact, however, an adequate fit to the data may be obtained by use of a simpler model in which the *d* and *g* states are viewed as comprising a single composite "reservoir" state. The model assumes that when the population of the parent *nf* state is much larger than that of the BB states a given BB peak is populated only by transitions from the parent *nf* state, and not by secondary transitions involving other BB produced states. The laser-produced atoms and the atoms comprising the BB features are assumed to decay with "effective" lifetimes that include the effects of spontaneous decay and BB-induced depopulation. The differential equation governing the population of the parent *nf* state is then

$$\frac{dN_0(t)}{dt} = -\frac{N_0(t)}{\tau_n}, \tag{1}$$

where $N_0(t)$ is the population of the parent *nf* state and τ_n its effective lifetime.

The time dependence of the total population $N_i(t)$ of the *i*th BB feature, which includes both *d* and *g* states, is given by

$$\frac{dN_i}{dt} = -\frac{N_i}{\tau_i} + \sum_j B_{0\to j}\,\rho(\nu_{0\to j})\,N_0$$

$$= -\frac{N_i}{\tau_i} + \frac{N_0}{\tau^*_{0\to i}}, \tag{2}$$

where τ_i is the effective composite lifetime for the atoms comprising the *i*th BB peak, $\rho(\nu)$ is the photon density, and $B_{0\to j}$ are the Einstein *B* coefficients for transitions to states *j* comprising the *i*th BB peak. Thus

$$\sum_j B_{0\to j}\,\rho(\nu_{0\to j}) = 1/\tau^*_{0\to i}$$

is the total transition rate, in inverse seconds, from the original *f* state to the *d* and *g* states which make up the *i*th BB peak.

Equations (1) and (2) have the solutions

$$N_0(t) = N_0(0)e^{-t/\tau_n}, \tag{3}$$

and

$$N_i(t) = N_0(0)e^{-t/\tau_n}\,\frac{1/\tau^*_{0\to i}}{1/\tau_i - 1/\tau_n}\left(1 - e^{(1/\tau_n - 1/\tau_i)t}\right). \tag{4}$$

The apparent lifetime of the parent *nf* state, τ_n, is measured in a subsidiary experiment, $\tau^*_{0\to i}$ and τ_i are adjusted to provide the best fit of Eq. (4) to the experimental data. As evident from Eq. (2), $1/\tau^*_{0\to i}$ is largely determined by the slope of the data at $t=0$. The inset in Fig. 2 shows the observed time dependence of a representative BB feature together with the best fit to the data obtained using this single reservoir model.

The measured ratios, R_{meas}, of the transition rates, from selected parent *nf* states, to the first three BB features at 300 and 90 K are shown in Table I. The corresponding ratios calculated by use of quantum-defect theory and BB spectral data are also included. Each BB feature comprises *d* and *g* states whose excitation requires different wavelengths. It is thus necessary to consider the excitation rate to each of these states, and its temperature dependence, separately, because the ratio of the BB-photon fluxes at 300 and 90 K is somewhat wavelength dependent over the range of interest. The matrix elements coupling the various initial and final states[17,18] were calculated using radial integrals determined by use of the quantum-defect technique.[19] These integrals agree well with those obtained by use of the data of Edmonds *et al.*[20] who have tabulated coefficients that can be used to calculate the electric dipole-matrix element between any two states whose effective principle quantum numbers differ by ten or less. The quantum defects used in the present calculations were estimated from published tabulations of atomic energy levels.[21] The average quantum defect

TABLE I. Effect of temperature on transition rates. R_{calc} and R_{meas} are the calculated and measured ratios of the transition rates, from selected parent *nf* states, to the first three BB peaks at 300 and 90 K.

Parent state	Product states	R_{calc}	R_{meas}
23*f*	24*g*, 26*d*	3.0	2.9 ± 0.6
	25*g*, 27*d*	3.3	4.0 ± 0.8
	26*g*, 28*d*	3.6	4.0 ± 0.8
25*f*	26*g*, 28*d*	2.9	3.0 ± 0.6
	27*g*, 29*d*	3.2	3.5 ± 0.7
	28*g*, 30*d*	3.4	3.3 ± 0.7
27*f*	28*g*, 30*d*	2.9	2.7 ± 0.6
	29*g*, 31*d*	3.1	2.8 ± 0.6
	30*g*, 32*d*	3.3	3.5 ± 0.8
29*f*	30*g*, 32*d*	2.9	2.8 ± 0.6
	31*g*, 33*d*	3.0	3.3 ± 0.7
	32*g*, 34*d*	3.2	3.0 ± 0.7

TABLE II. Measured and calculated transition rates for BB-induced photoexcitation. Calculated transition rates from selected parent nf atoms to the d and g states comprising individual SFI features are shown together with the total calculated transition rate to each feature. The corresponding measured transition rates are also included.

Parent f state	Product g state	Calculated transition rates (sec^{-1}) $1/\tau^*_{0\to g}$	Product d state	$1/\tau^*_{0\to d}$	$1/\tau^*_{0\to t}$	Measured transition rates[a] (sec^{-1}) $1/\tau^*_{0\to t}$
20f	21g	3224	23d	4866	8090	7500^{+1500}_{-2300}
	22g	1602	24d	994	2596	2400 ± 500
	23g	980	25d	464	1444	1300 ± 300
24f	25g	2110	27d	3567	5677	7500^{+1500}_{-2300}
	26g	1075	28d	749	1824	2000 ± 400
	27g	674	29d	359	1033	1100 ± 200
25f	26g	1919	28d	3321	5240	7500^{+1500}_{-2300}
	27g	981	29d	701	1622	1800 ± 400
	28g	618	30d	338	956	1100 ± 200

[a] Measured rates are obtained assuming that BB produced d and g atoms ionize adiabatically.

for the relevant states in the d series is 2.43, and for the f series, 0.056. In the absence of data for the g series, they are assumed to have a quantum defect of zero. The good agreement between the calculated and measured ratios provides further confirmation that the observed effects are due to photoexcitation by background BB radiation.

The good agreement between the calculated and observed transition rates at 300 K, shown in Table II, indicates that, for xenon, quantum-defect theory provides reliable matrix elements. It should be noted that the measured rates presented in Table II are obtained assuming that the d and g states ionize adiabatically. Previous studies of xenon have shown that, for the range of n of interest, states with $|m_l| \leq 3$ ionize predominantly adiabatically. However, even if those g states that yield high-field states with $|m_l| = 4$ were to ionize diabatically, and thus not be included in the measured BB features, this would introduce an error of only ~10% in the measured total BB population.

In addition to SFI features resulting from photoexcitation, features arising from blackbody induced photodeexcitation (stimulated emission) have also been observed. The transition rates to these states are again in agreement with those expected on the basis of quantum-defect theory.

ACKNOWLEDGMENTS

We wish to thank F. G. Kellert and G. W. Foltz for many helpful discussions. This material is based on work supported by the National Science Foundation under Grant No. PHY 78-09860 and the Robert A. Welch Foundation. One of us (G.J.H.) acknowledges additional support by the Department of Energy, Office of Basic Energy Sciences.

[1]E. J. Beiting, G. F. Hildebrandt, F. G. Kellert, G. W. Foltz, K. A. Smith, F. B. Dunning, and R. F. Stebbings, J. Chem. Phys. 70, 3551 (1979).
[2]T. F. Gallagher and W. E. Cooke, Phys. Rev. Lett. 42, 835 (1979).
[3]T. W. Ducas, W. P. Spencer, A. G. Vaidyanathan, W. H. Hamilton, and D. Kleppner, Appl. Phys. Lett. 35, 382 (1979).
[4]T. F. Gallagher and W. E. Cooke, Appl. Phys. Lett. 34, 370 (1979).
[5]W. E. Cooke and T. F. Gallagher, Phys. Rev. A 21, 588 (1980).
[6]F. Gounand, M. Hugon, P. R. Fournier, and J. Berlande, J. Phys. B 12, 547 (1979).
[7]M. Gross, P. Goy, C. Fabre, S. Haroche, and J. M. Raimond, Phys. Rev. Lett. 43, 343 (1979).
[8]P. R. Koch, H. Hieronymus, A. F. J. von Raan, and W. Raith, Phys. Lett. 75A, 273 (1980).
[9]H. Figger, G. Leuchs, R. Straubinger, and H. Walther, Opt. Commun. 33, 37 (1980).
[10]F. G. Kellert, K. A. Smith, R. D. Rundel, F. B. Dunning, and R. F. Stebbings, J. Chem. Phys. 72, 3179 (1980).
[11]R. F. Stebbings, C. J. Latimer, W. P. West, F. B.

Dunning, and T. B. Cook, Phys. Rev. A 12, 1453 (1975).
[12]T. H. Jeys, G. W. Foltz, K. A. Smith, E. J. Beiting, F. G. Kellert, F. B. Dunning, and R. F. Stebbings, Phys. Rev. Lett. 44, 390 (1980).
[13]F. G. Kellert, T. H. Jeys, K. A. Smith, F. B. Dunning, and R. F. Stebbings, J. Chem. Phys. 72, 6312 (1980).
[14]M. G. Littman, M. M. Kash, and D. Kleppner, Phys. Rev. Lett. 41, 103 (1978).
[15]T. F. Gallagher, L. M. Humphrey, W. E. Cooke, R. M. Hill, and S. A. Edelstein, Phys. Rev. A 16, 1098 (1977).
[16]T. H. Jeys, K. A. Smith, F. B. Dunning, and R. F. Stebbings, Phys. Rev. A 23, 3065 (1981).
[17]G. F. Koster and H. Statz, J. Appl. Phys. 32, 2054 (1961).
[18]H. Statz, C. L. Tang, and G. F. Koster, J. Appl. Phys. 34, 2625 (1963).
[19]D. R. Bates and A. Damgaard, Philos. Trans. R. Soc. London, Ser. A 242, 101 (1949); F. Gounand, J. Phys. (Paris) 40, 457 (1979).
[20]A. R. Edmonds, J. Picart, N. T. Minh, and R. Pullen, J. Phys. B 12, 2781 (1979).
[21]C. E. Moore, *Atomic Energy Levels*, NBS Circular No. 467 (U. S. GPO, Washington, D. C., 1958), Vol. III.